

A Single Scale Doesn't Fit All: Adaptive Motion Scaling for Efficient and Precise Teleoperation

Jeonghyeon Yoon^{1*}, Sanghyeok Park^{2*}, Hyojae Park¹, Cholin Kim¹, Sihyeoung Park¹, and Minho Hwang^{1†}

Abstract—Teleoperation is increasingly employed in environments where direct human access is difficult, such as hazardous exploration or surgical field. However, if the motion scale factor(MSF) intended to compensate for workspace-size differences is set inappropriately, repeated clutching operations and reduced precision can significantly raise cognitive load. This paper presents a shared controller that dynamically applies the MSF based on the user's intended motion scale. Inspired by human motor skills, the leader arm trajectory is divided into coarse(fast, large-range movements) and fine(precise, small-range movements), with three features extracted to train a fuzzy C-means(FCM) clustering model that probabilistically classifies the user's motion scale. Scaling the robot's motion accordingly reduces unnecessary repetition for large-scale movements and enables more precise control for fine operations. Incorporating recent trajectory data into model updates and offering user feedback for adjusting the MSF range and response speed allows mutual adaptation between user and system. In peg transfer experiments, compared to using a fixed single scale, the proposed approach demonstrated improved task efficiency(number of clutching and task completion time decreased 38.46% and 11.96% respectively), while NASA-TLX scores confirmed a meaningful reduction(58.01% decreased) in cognitive load. This outcome suggests that a user-intent-based motion scale adjustment can effectively enhance both efficiency and precision in teleoperation.

I. INTRODUCTION

Telerobotics is a technology that extends human operational capabilities by combining human cognitive and intelligent decision-making abilities with the execution of robot's motion. Through this technology, robots can be remotely operated to perform various tasks in environments that are difficult for humans to access, such as extreme environment exploration or disaster rescue missions [1], [2]. In the medical field, it also contributes to shorter patient recovery times by enabling minimally invasive surgery [3], [4].

During teleoperation, the operator acquires information from the remote environment through a user interface while simultaneously transmitting control commands to the robot. This process increases the operator's cognitive load. In teleoperation systems, operators receive real-time multisensory feedback—such as visual, haptic, force, and auditory cues—through the user interface. They must process these sensory inputs simultaneously to assess the situation while

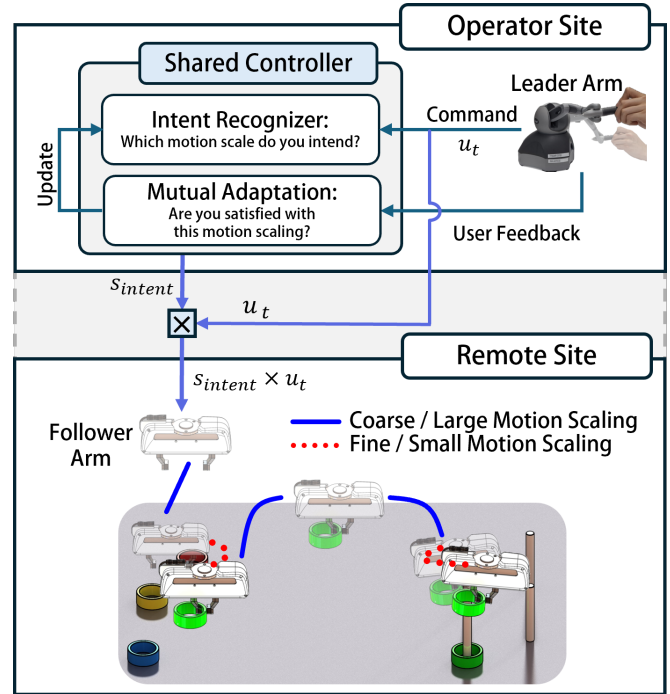


Fig. 1. **System Overview:** User operates the robot remotely via the leader arm. **Intent Recognizer:** The shared controller classifies the user's motion as coarse or fine based on the leader arm's input(u_t), dynamically adjusting the motion scaling factor(s_{intent}). **Mutual Adaptation:** The system receives real-time feedback on scaling adjustments, refining the Intent Recognizer for personalized control, enhancing user experience.

also managing control inputs via haptic devices, pedals, and gripper actuation buttons. This complex information processing significantly increases cognitive load, reducing focus and ultimately decreasing task efficiency [5], [6].

Moreover, when there is a workspace discrepancy between the remote site and the operator site(e.g. micro-surgery), a motion scale factor(MSF) is applied to scale the motion commands up or down, compensating for the difference. However, improper MSF settings can hinder the operator's control ability [7], [8]. For instance, if the MSF is too small, the operator must frequently clutch to perform multiple motion indexing steps to reach the target, reducing task efficiency. Conversely, if the MSF is too large, small movements are excessively amplified, decreasing control precision and increasing the likelihood of the target positioning errors. Therefore, careful MSF design is crucial to minimize cognitive load while ensuring an optimal teleoperation experience.

This paper proposes a shared controller that dynamically adjusts the MSF in real-time based on the user's intended motion scale. Human motor skills can be classified as

* Equal Contribution, † Corresponding author

¹Jeonghyeon Yoon, Hyojae Park, Cholin Kim, Sihyeoung Park, and Minho Hwang are with the Department of Robotics and Mechatronics Engineering, DGIST, Daegu, 42988, Republic of Korea {yjh1434, hyojae, cholin, psh120, minho}@dgist.ac.kr

²Sanghyeok Park is with the School of Undergraduate Studies, DGIST, Daegu, 42988, Republic of Korea sh.park@dgist.ac.kr

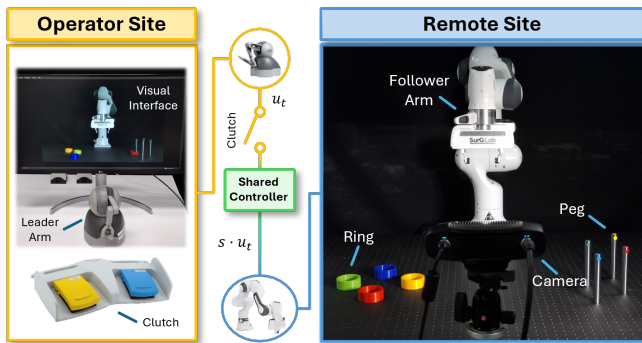


Fig. 2. **Teleoperation System Setup:** The user controls the robot remotely via the leader arm while viewing a camera feed. The leader arm sends commands(u_t), and the clutch manages motion indexing by connecting or disconnecting inputs. The shared controller determines the MSF, applying a scaled command($s \cdot u_t$) to the robot.

gross(large, fast movements) or fine(small, precise movements) [9]. A key aspect of fine motor skills is that they often rely on human sensory feedback(e.g. tactile, visual) for real-time corrections. Inspired by this mechanism, the proposed shared controller utilizes the leader arm’s trajectory to adaptively modify the MSF during teleoperation.

An overview of the proposed shared controller is illustrated in Fig. 1. The shared controller operates in two stages. In Stage 1, the system classifies the operator’s intended motion scale as coarse or fine based on the leader arm’s trajectory and applies the appropriate scaling to the follower arm’s motion commands. In Stage 2, the operator provides feedback to the shared controller, allowing the system to adapt and update accordingly. While previous studies focused on generalizing the adjustment process [10] [11], this study focuses on dynamically adjusting the MSF in real-time based on the recognition of the intended motion scale by the operator. The main contributions of the proposed shared controller are as follows:

- Features are extracted from the user’s control input to classify the intended motion scale and designed an intent recognizer using fuzzy C-means clustering.
- Mutual adaptation is implemented, where user feedback on the shared controller is used to update the parameters of the intent recognizer.
- Experimental results from the peg transfer task showed that the proposed shared controller outperformed fixed MSF settings in both task performance and workload reduction.

II. RELATED WORKS

Various approaches have been explored to reduce the cognitive load in telerobotics. Telepresence enhances user immersion by simulating physical presence through control and display technologies [12], [13], improving efficiency by reducing cognitive load and task execution time. Audonnet et al. [14] proposed a mixed reality digital twin framework integrating VR, while Ponomareva et al. [15] leveraged R-CNN in augmented environments to improve remote precision. Both methods reduced operator workload, with the

latter also optimizing execution time and movement paths.

Shared control strategies have also demonstrated cognitive load reduction and performance improvements. Zhu et al. [16] applied template-based point cloud compensation to enhance multi-angle grasping and implemented shared control, reducing task time and improving precision. Pérez-D’Arpino et al. [17] employed State-Guidance Shared Control with assisted planning, increasing accuracy in structured tasks while decreasing operator effort. Menon et al. [18] developed a user-adaptive multi-layer shared control predicting user actions with over 92% accuracy while also tracking and mitigating user fatigue.

For task-specific shared control, Han et al. [19] applied dependent shared control in dual-arm nuclear power plant teleoperation, reducing cognitive load and task time. Han et al. [20] introduced virtual links and obstacle avoidance algorithms, improving efficiency for both skilled and unskilled users. Bowman et al. [21] addressed human-robot hand discrepancies, developing a shared control strategy that ensured stable grasping by balancing robotic assistance with human intent.

Research has also been conducted on dynamically changing the Motion Scaling Factor(MSF). Richter et al. [10] proposed a dynamic MSF setting method to improve the performance of remote robotic surgery systems under network delay during the teleoperation process. Hsia et al. [11] modeled leader-follower teleoperation as a human-in-loop control system and determined the MSF through filter design. These studies commonly proposed a generalized method to dynamically change the MSF. This paper proposes a user-customized MSF setting method that identifies the motion scale intended by the user and adjusts the MSF based on the user’s adaptability.

III. SHARED CONTROL ARCHITECTURE

The operator uses a leader arm with a clutch to teleoperate the remote robot, while receiving real-time visual feedback from a camera feed(Fig. 2). Because the operator’s workspace and the robot’s workspace differ in scale, the robot’s motions are commanded through a scaled trajectory using a motion scaling factor(MSF). A shared controller is proposed to dynamically adjust this MSF based on user intent and the user’s adaptation level. The shared controller consists of two main components: 1) Intent Recognizer that infers the user’s intended scale in real-time, and 2) Mutual Adaptation mechanism that updates control parameters as the user adapts.

A. Intent Recognizer

The Intent Recognizer classifies the user’s intended motion scale using leader arm trajectory data(Figure Fig. 3, green part). While the clutch is pressed, three key features—speed, alignment, and displacement—are extracted from the trajectory. These features are then processed by a pre-trained Fuzzy C-Means(FCM) clustering model, which classifies the motion scale as coarse or fine. The predicted MSF is refined using a low-pass filter(LPF) to ensure smooth application.

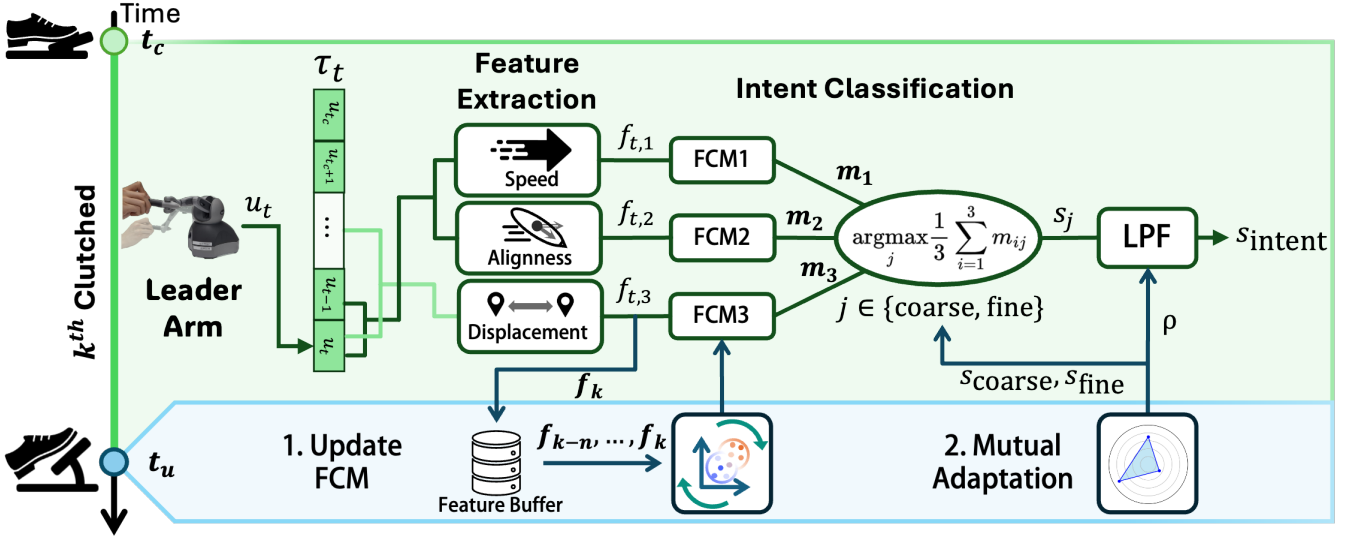


Fig. 3. **Systematic Diagram of Shared Controller:** The shared controller classifies the user’s intent(coarse or fine) based on Leader Arm inputs and dynamically adjusts the motion scaling factor(MSF). **Clutched Phase(from t_c to t_u , Green Region):** The leader arm generates a trajectory(τ_t) from real-time position commands(u_t). Three key features—speed, alignment, and displacement($f_{t,i}$)—are extracted and processed through pre-trained fuzzy C-means clustering(FCM) models, which output the probability(m_i) of the motion being coarse or fine. The final MSF(s_j) is determined by averaging these probabilities, then refined using a low-pass filter(LPF) to produce the final scaling factor(s_{intent}). This process runs at 100 Hz while the user is clutching. **Unclutched Phase(t_u , Blue Region):** Once the clutch is released, the trajectory’s extracted features(f_k) are stored in a buffer. The FCM model is updated using the most recent n feature samples. Additionally, through the mutual adaptation interface, the user can adjust the scaling boundaries(s_{coarse} , s_{fine}) and the LPF’s convergence speed(ρ) for personalized control. The system continuously updates based on both trajectory data and user feedback, ensuring adaptive optimization over time.

TABLE I
FEATURES OF MOTION SCALE

Features	Coarse Motion	Fine Motion
Speed	High	Low
Alignnness	≈ 0	≈ 1
Displacement	High	Low

* v : velocity of the leader arm’s end-effector.

* \hat{u}_{tool} : unit vector from the follower arm’s end-effector to the tool tip.

* Δx : displacement of the leader arm’s end-effector.

This process runs continuously while the clutch is engaged, allowing real-time MSF adjustments based on user intent.

1) *Feature Extraction:* Human motor behavior tends to differ when performing large motions versus delicate precise motions [9]. For example, moving the robot a long distance prompts the user to make faster and larger movements with the leader arm, whereas precise alignment tasks involve slower, meticulous adjustments. Based on such observations, three key features are defined to distinguish coarse vs. fine motion scales intended to be task-agnostic, though specific tasks might use additional features:

- Speed – Fine motions are typically slow(due to frequent minor corrections), whereas coarse motions involve higher speeds.
- Alignnness – This measures alignment between the leader’s velocity vector and the tool’s orientation. Fine motion tends to maintain a consistent tool direction(high alignment), whereas coarse motion is less constrained

in direction changes.

- Displacement over a short window – Fine motion consists of many small back-and-forth adjustments(lower net displacement), while coarse motion covers a greater distance in the same time span.

These features are computed over the recent trajectory while the clutch is held. Although the chosen features worked across experimental tasks of this paper, certain applications may require custom feature definitions for optimal intent classification.

2) *Intent Classification:* To classify motion scale based on extracted features, the Fuzzy C-Means(FCM) clustering algorithm [22] is applied to the last n trajectory samples. Unlike hard clustering methods, FCM assigns probabilistic memberships, allowing for a more flexible classification of user intent. Given that user behavior varies, FCM enables adaptive classification instead of relying on fixed decision boundaries.

FCM minimizes the following objective function J :

$$J = \sum_{i=1}^N \sum_{j=1}^2 u_{ij}^m \|f_{t,i} - c_j\|^2 \quad (1)$$

where u_{ij} represents the membership probability of data point $f_{t,i}$ belonging to cluster c_j . The update rules for membership probability and cluster centers are given by

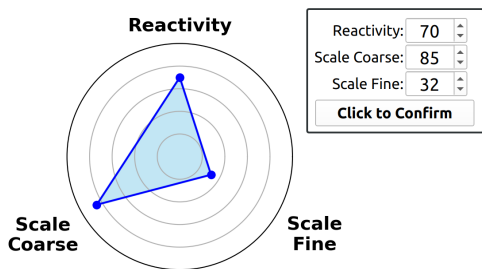


Fig. 4. **Mutual Adaptation Interface:** Through this interface, users can update parameters by adjusting the MSF change rate(Reactivity) and the MSF range(Scale Coarse and Fine).

$$u_{ij} = \frac{1}{\sum_{k=1}^C \left(\frac{\|f_{t,i} - c_j\|}{\|f_{t,i} - c_k\|} \right)^{\frac{2}{m-1}}}, \quad c_j = \frac{\sum_{i=1}^N u_{ij}^m f_{t,i}}{\sum_{i=1}^N u_{ij}^m} \quad (2)$$

Each feature is processed by an individual FCM model, and the final MSF classification is determined by averaging the membership values across all three models. The selected MSF is then smoothed using a discrete LPF:

$$\operatorname{argmax}_j \frac{1}{3} \sum_{i=1}^3 u_{ij}, \quad \text{where } j \in \{\text{coarse, fine}\} \\ s_{\text{intent}} = (1 - \rho)s_{\text{prev}} + \rho s_j \quad (3)$$

where ρ controls the reactivity of the LPF, determining how quickly the predicted MSF is applied.

B. Mutual Adaptation: System Update Strategy

Humans naturally adapt to new systems and environments [23]. To enhance adaptability, the shared controller incorporates two system update strategies.

The first component is an adaptive intent recognition. The FCM model is updated immediately after the clutch is released, using only the most recent n leader arm trajectories. This ensures that the system adapts to user behavior over time. The second component is Mutual Adaptation Interface, which is optional. Users may manually adjust key control parameters for personalization. However, experimental results suggest that performance was slightly better without user intervention. Therefore, updating control parameters remains optional. The interface is designed with reference to [24]. The Mutual Adaptation Interface (Figure 4) allows users to adjust:

- Reactivity(ρ): Controls discrete LPF convergence speed(eq. (3)).
- MSF Bounds($s_{\text{coarse}}, s_{\text{fine}}$): Defines upper and lower MSF limits.

The final parameters are normalized via denormalization:

$$\theta = \tilde{\theta} \odot (\theta_{\max} - \theta_{\min}) + \theta_{\min}, \\ \text{where } \theta = \begin{bmatrix} \rho & s_{\text{fine}} & s_{\text{coarse}} \end{bmatrix}^T. \quad (4)$$

Where $\tilde{\theta}$ and θ represents the normalized value produced from interface and updated intent recognizer parameters

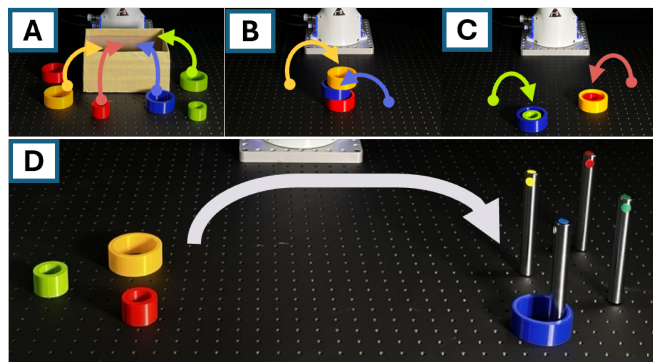


Fig. 5. **Training and Evaluation:** Volunteers undergo training(A: box placement, B: ring stacking, C: ring-in-ring) before testing the shared controller. Performance is then evaluated through the Peg Transfer task(D).

each, ensuring they remain within hardware constraints. \odot denotes element-wise multiplication.

This mutual adaptation mechanism allows the system to evolve alongside the user, while also providing an optional customization interface for those who prefer manual tuning.

IV. EXPERIMENT AND RESULT

To evaluate the proposed shared controller, the user controls the remote follower arm via a leader arm and clutch while receiving visual feedback(Fig. 2). The experiment involves performing a peg transfer task(Fig. 5(D)), where four rings must be placed onto pegs of matching colors. Performance is compared between a fixed MSF and the proposed method.

A. Experiment

The peg transfer task is a fundamental exercise in laparoscopic surgery training, designed to test the operator's precision, hand-eye(visuomotor) coordination, and bimanual dexterity [25]. In the teleoperation setup, a Geomagic Touch haptic device(3D Systems) served as the leader arm, while a Franka Emika Panda robot(Franka Robotics) acted as the follower arm. Four rings of different colors and two sizes were used as objects to transfer onto matching pegs. The size variation was intentional – smaller rings demand much more delicate fine motor control compared to larger ones. Since the task itself is simply placing rings onto designated pegs, it is straightforward for even non-experts to understand, making it ideal for experimentation.

The subjects consist of three volunteers who have no experience with teleoperation but possess general knowledge of robotics. Before attempting the main task, participants underwent a training phase with three preliminary tasks(Fig. 5, A–C) to familiarize themselves with the teleoperation system. After this practice, each participant performed the peg transfer task three times(Fig. 5, D) under three different conditions to assess performance:

- 1) Fixed MSF: The MSF remains constant to 1 and 3.
- 2) Shared Controller(w/o MA): The MSF dynamically changes based on the user's inferred motion scaling intent. MA represents Mutual Adaptation(control parameter update) using the interface.

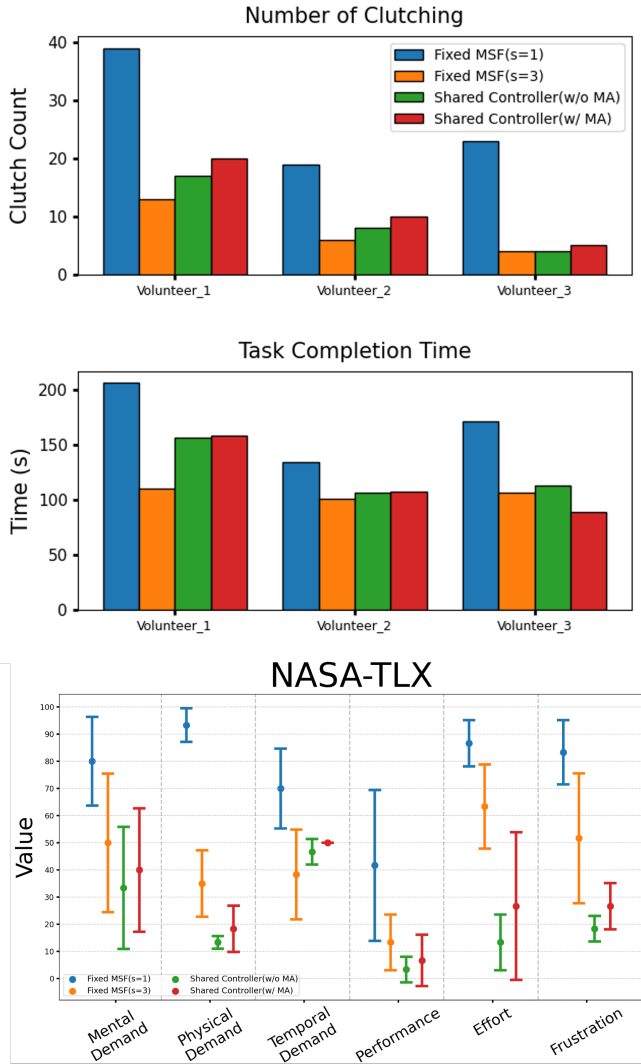


Fig. 6. **Performance Assessment and NASA-TLX** The figure compares performance assessment (clutching count, task completion time), and NASA-TLX scores across different MSF settings. The proposed shared controller achieves a balance by greatly reducing clutch frequency and task time versus the low fixed scale ($s = 1$), while maintaining reasonable completion time with much lower workload than the high fixed scale ($s = 3$). Both adaptive approaches (Shared Controller(w/o MA) and Shared Controller(w/ MA) outperform the fixed scaling settings in efficiency and reduced operator workload.

- 3) Shared Controller(w/ MA): Alongside the intent recognition, the user optimizes control parameters empirically using mutual adaptation.

Each trial was evaluated using three key performance metrics:

- Task Completion Time(TCT): The time required to complete the peg transfer task.
- Number of Clutching(N_{clutch}): The total number of clutch(re-centering) button presses during the task.
- NASA Task Load index(TLX): A subjective workload measure – lower scores indicate lower perceived cognitive load [26].

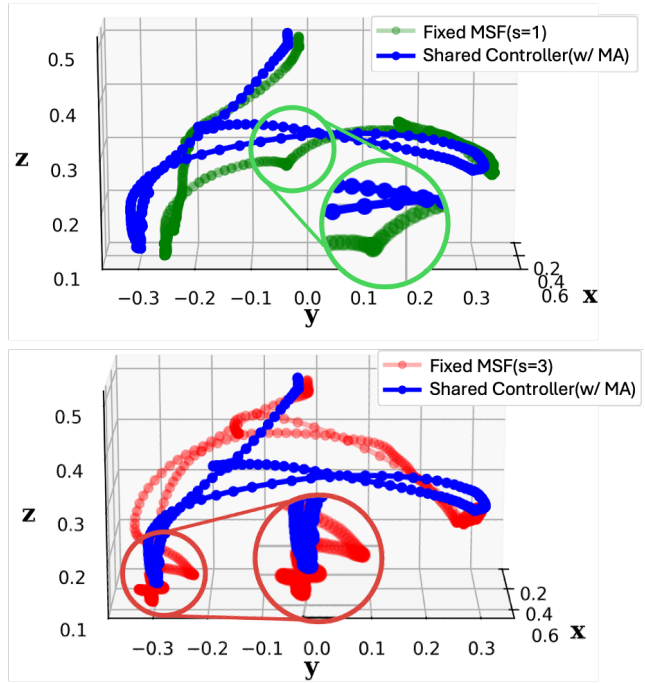


Fig. 7. **Follower arm trajectory: Fixed MSF vs. Shared controller:** A low, fixed MSF(upper, green) requires frequent clutching(motion indexing), resulting in unnecessary trajectories. A high, fixed MSF(lower, red) exacerbates tremors in fine tasks. In contrast, the proposed shared controller(right, blue) dynamically adjusts the MSF to alleviate both issues.

B. Result

The proposed shared controller is evaluated using a standard peg transfer task under various motion scaling factor(MSF) conditions. The goal was to compare task performance and user workload between the proposed shared controller and fixed scaling settings. Fig. 6 illustrates the results in terms of task completion time(TCT), number of clutching actions(N_{clutch}), and NASA-TLX subjective workload scores for each method.

1) Fixed MSF vs. Proposed Method: Compared to Fixed MSF($s = 1$), the proposed method significantly improved efficiency. Shared Controller(w/o MA) reduced N_{clutch} by 65.64% and TCT by 26.36%. Shared Controller(w/ MA) reduced N_{clutch} by 58.12% and TCT by 30.47%. These reductions indicate that the adaptive controller minimized excessive clutching and allowed smoother task execution.

Compared to Fixed MSF($s = 3$), the proposed method showed N_{clutch} increased by 21.37%(Shared Controller(w/o MA)) and 48.50%(Shared Controller(w/ MA)). TCT increased by 17.73%(Shared Controller(w/o MA)) and 11.18%(Shared Controller). While Fixed MSF($s = 3$) resulted in faster task completion, its excessive scaling compromised control stability. During experiments, despite the participants having sufficient training, the robot encountered singularities and collisions an average of 3.3 and 2.0 times per trial, highlighting the risks of over-amplified motions in high-scale settings. In contrast, the proposed method maintained greater control precision(without any singularities or collisions) while still reducing cognitive workload.

2) Shared Controller(w/o MA) vs. Shared Controller(w/

MA): Shared Controller(w/o MA) outperformed Shared Controller(w/ MA) slightly, requiring 17.14% fewer clutch presses and resulting in an average 23% lower workload in NASA-TLX. The Shared Controller provided a more adaptive experience, but empirical control parameter updates increased cognitive load, leading to slightly higher clutching frequency and task completion time.

3) Trajectory Efficiency: An interesting observation from the experiment is that the proposed shared controller helps users generate more efficient trajectories. Fig. 7 compares trajectories under different MSF settings. With a fixed MSF of 1(green), frequent clutching results in repetitive movements, lowering efficiency. A fixed MSF of 3(red) excessively amplifies small motions, leading to jittering and reduced precision. In contrast, the proposed shared controller(blue) dynamically adjusts the MSF based on user intent, reducing unnecessary clutching and preventing over-amplification, ultimately improving both efficiency and precision in teleoperation.

V. CONCLUSIONS

The proposed shared controller effectively demonstrated an adaptive approach to motion scaling in teleoperation, addressing the limitations of fixed MSF settings. Human motor skills were analyzed, and a user intention recognition model was designed based on this analysis. Additionally, for mutual adaptation between the shared controller and the user, only a few recent trajectories were utilized, and the system was updated through user feedback. Through the peg transfer experiment, the results revealed that the system reduced excessive motion during large-scale movements while enhancing precision in fine-scale operations. Compared to fixed scaling factors, the adaptive controller minimized the need for repeated clutching, with the number of clutching decreasing by 38.46%, and improved task efficiency, reducing task completion time by 11.96%. Additionally, the system delivered a more intuitive teleoperation experience. Moreover, NASA-TLX scores across all metrics indicated that the proposed method not only enhanced task performance but also significantly reduced cognitive load, with a 58.01% decrease compared to using a fixed single scale.

Despite these advantages, the system exhibits some limitations. Although the motion classification feature set was designed to balance generality and specificity, certain features may not be universally applicable across all tasks. Expanding feature diversity and refining classification techniques could further improve adaptability. Additionally, experiments revealed that manual control parameter updates increased workload and slightly reduced performance. Future research should focus on automating control parameter adjustments to eliminate the need for user intervention, thereby further enhancing efficiency, precision, and overall user experience in teleoperation systems.

ACKNOWLEDGMENT

This work was supported by Korea Medical Device Development Fund grant funded by the Korea government

(1711196477, RS-2023-00252244), the National Research Council of Science & Technology(NST) grant funded by the Korea government(MSIT)(CRC23021-000), the Industrial Strategic Technology Development Program(ISTDP)(RS-2024-00443054) funded by the Ministry of Trade, Industry & Energy(MOTIE, Korea), and by the collaborative project with ROEN Surgical Inc.

REFERENCES

- [1] M. A. Goodrich and A. C. Schultz, *Human-Robot Interaction: A Survey*. 2008.
- [2] H. Yamada, N. Tao, and Z. DingXuan, "Construction tele-robot system with virtual reality," in *2008 IEEE Conference on Robotics, Automation and Mechatronics*, 2008, pp. 36–40.
- [3] G. Guthart and J. K. Salisbury, "The intuitive/sup tm/ telesurgery system: overview and application," *Proceedings 2000 ICRA. Millennium Conference. IEEE International Conference on Robotics and Automation. Symposia Proceedings (Cat. No.00CH37065)*, vol. 1, pp. 618–621 vol.1, 2000.
- [4] N. Simaan, K. Xu, A. Kapoor, W. Wei, P. Kazanzides, P. Flint, and R. Taylor, "Design and integration of a telerobotic system for minimally invasive surgery of the throat," *The International Journal of Robotics Research*, vol. 28, no. 9, pp. 1134–1153, 2009.
- [5] J. Du, W. Vann, T. Zhou, Y. Ye, and Q. Zhu, "Sensory manipulation as a countermeasure to robot teleoperation delays: system and evidence," *Scientific Reports*, vol. 14, no. 1, p. 4333, Feb. 2024.
- [6] J. Pan, J. Eden, D. Oetomo, and W. Johal, "Effects of shared control on cognitive load and trust in teleoperated trajectory tracking," *IEEE Robotics and Automation Letters*, vol. 9, pp. 5863–5870, 2024.
- [7] B. Omarali *et al.*, "Position and velocity control for telemanipulation with interoperable teleoperation protocol," in *2019 IEEE International Conference on Systems, Man and Cybernetics (SMC)*, 2019, pp. 4281–4286.
- [8] B. Omarali, S. Javaid, M. Valle, and I. Farkhatdinov, "Workspace scaling in virtual reality based robot teleoperation," in *Proceedings of the Augmented Humans International Conference 2023*, 2023, p. 98–104.
- [9] M. Matheis and J. A. Estabillio, "Assessment of fine and gross motor skills in children," *Handbook of childhood psychopathology and developmental disabilities assessment*, pp. 467–484, 2018.
- [10] F. Richter, R. K. Orosco, and M. C. Yip, "Motion scaling solutions for improved performance in high delay surgical teleoperation," in *2019 International Conference on Robotics and Automation (ICRA)*, 2019, pp. 1590–1595.
- [11] S.-K. Hsia, Y.-H. Chuang, and C.-W. Chen, "Auto-tuned motion scaling in teleoperation based on human reaction model identification," *IEEE Robotics and Automation Letters*, vol. 7, no. 1, pp. 318–325, 2022.
- [12] A. J. Fairchild, S. P. Campion, A. S. García, R. Wolff, T. Fernando, and D. J. Roberts, "A mixed reality telepresence system for collaborative space operation," *IEEE Transactions on Circuits and Systems for Video Technology*, vol. 27, no. 4, pp. 814–827, 2016.
- [13] J. V. Draper, D. B. Kaber, and J. M. Usher, "Telepresence," *Human Factors*, vol. 40, no. 3, pp. 354–375, 1998, pMID: 9849099. [Online]. Available: <https://doi.org/10.1518/001872098779591386>
- [14] F. P. Audonnet, I. G. Ramirez-Alpizar, and G. Aragon-Camarasa, "Immertwin: A mixed reality framework for enhanced robotic arm teleoperation," *arXiv preprint arXiv:2409.08964*, 2024.
- [15] P. Ponomareva, D. Trinitatova, A. Fedoseev, I. Kalinov, and D. Tsetserukou, "Grasplook: a vr-based telemanipulation system with r-cnn-driven augmentation of virtual environment," in *2021 20th International Conference on Advanced Robotics (ICAR)*. IEEE, 2021, pp. 166–171.
- [16] Y. Zhu, B. Jiang, Q. Chen, T. Aoyama, and Y. Hasegawa, "A shared control framework for enhanced grasping performance in teleoperation," *IEEE Access*, vol. 11, pp. 69 204–69 215, 2023.
- [17] C. Pérez-D'Arpino, R. P. Khurshid, and J. A. Shah, "Experimental assessment of human-robot teaming for multi-step remote manipulation with expert operators," *ACM Transactions on Human-Robot Interaction*, vol. 13, no. 3, pp. 1–26, 2024.

- [18] A. Menon, L. I. G. Olascoaga, V. Balanaga, A. Natarajan, J. Ruffing, R. Ardalán, and J. M. Rabaey, "Shared control of assistive robots through user-intent prediction and hyperdimensional recall of reactive behavior," in *2023 IEEE International Conference on Robotics and Automation (ICRA)*. IEEE, 2023, pp. 12 638–12 644.
- [19] J. Han and G.-H. Yang, "Improving teleoperator efficiency using position–rate hybrid controllers and task decomposition," *Applied Sciences*, vol. 12, no. 19, p. 9672, 2022.
- [20] J. Han, K. Cho, I. Jang, C. Ju, H. Il Son, and G.-H. Yang, "Development of a shared controller for obstacle avoidance in a teleoperation system," *International Journal of Control, Automation and Systems*, vol. 18, no. 11, pp. 2974–2982, 2020.
- [21] M. Bowman, J. Zhang, and X. Zhang, "Intent-based task-oriented shared control for intuitive telemanipulation," *Journal of Intelligent & Robotic Systems*, vol. 110, no. 4, pp. 1–24, 2024.
- [22] J. C. Bezdek, R. Ehrlich, and W. Full, "Fcm: The fuzzy c-means clustering algorithm," *Computers & geosciences*, vol. 10, no. 2-3, pp. 191–203, 1984.
- [23] E. F. Moran, *Human adaptability: An introduction to ecological anthropology*. Routledge, 2022.
- [24] R. Luo, M. Zolotas, D. Moore, and T. Padir, "User-customizable shared control for robot teleoperation via virtual reality," in *2024 IEEE/RSJ International Conference on Intelligent Robots and Systems (IROS)*, 2024, pp. 12 196–12 203.
- [25] D. R. Cullinan, M. R. Schill, A. DeClue, A. Salles, P. E. Wise, and M. M. Awad, "Fundamentals of laparoscopic surgery: Not only for senior residents," *Journal of Surgical Education*, vol. 74, no. 6, pp. e51–e54, 2017. [Online]. Available: <https://www.sciencedirect.com/science/article/pii/S1931720417302507>
- [26] S. G. Hart and L. E. Staveland, "Development of nasa-tlx (task load index): Results of empirical and theoretical research," *Human mental workload*, vol. 1, no. 3, pp. 139–183, 1988.